

Hyperfine structure and Λ doubling in the $A^2\Delta$ state of CH: Observation of an internal hyperfine perturbation

Wim Ubachs, W. M. van Herpen, J. J. ter Meulen, and A. Dymanus

Fysisch Laboratorium, Katholieke Universiteit Nijmegen, The Netherlands

(Received 27 January 1986; accepted 5 March 1986)

We report the observation of a resonance between hyperfine states, due to the crossing of rotational ladders at $N = 10$ of $\Delta_{5/2}$ and $\Delta_{3/2}$ spin-doublet states in the excited $A^2\Delta$ state of CH. Accurate values for the hyperfine constants a , b , and c in the $A^2\Delta$ state were obtained. From measurements of the Λ -doublet splittings we estimate an upper limit to the Λ doubling in the $A^2\Delta$ state.

I. INTRODUCTION

The rotational, Λ -doubling, and hyperfine structure of the $X^2\Pi$ ground state of the free radical carbon hydride (CH) have been well established by interstellar^{1,2} and laboratory^{3,4} microwave spectroscopy and by laser magnetic resonance at far infrared wavelengths.⁵ The rotational structure of the $A^2\Delta$ state was known from the optical emission spectrum of the $A^2\Delta-X^2\Pi$ system at $\lambda = 430$ nm.⁶ Recently Brazier and Brown⁴ performed high resolution laser spectroscopy on the $A^2\Delta-X^2\Pi$ transition, using the saturation technique of intermodulated fluorescence. They were able to resolve the hyperfine structure in the $A^2\Delta$ state, due to the nuclear spin of the proton and they measured hyperfine splittings in both F_1 ($\Delta_{5/2}$ state) and F_2 ($\Delta_{3/2}$ state) ladders for $N = 2$ to $N = 5$.

In the present paper we report the exact hyperfine structure in the $A^2\Delta$ state for N up to 14. For $N = 10$ a hyperfine resonance was observed: the hyperfine splittings are twice as large as expected from the hyperfine constants given by Brazier and Brown⁴ and additional lines appeared in the spectra. The hyperfine perturbations are shown to be caused by a crossing of F_1 and F_2 rotational ladders. Similar perturbations have been observed in electronic Σ states of VO^{7-9} and could be described by a magnetic hyperfine interaction between the electron spin multiplet states. A different kind of hyperfine resonance was observed in the $A^6\Sigma^+$ state of MnO ,¹⁰ where the perturber is a high vibronic state $v = 25$ of the electronic ground state $X^6\Sigma^+$. To our knowledge the present observation is the first example of a hyperfine resonance within an electronic state that is not of Σ type.

The Λ splittings in F_1 and F_2 ladders of the $A^2\Delta$ state were derived by Brazier and Brown⁴ from differences of absolute frequencies of $A^2\Delta-X^2\Pi$ rotational transitions for N values higher than 6, measured with lower (Doppler limited) resolution. The accuracy in the experimental values of these splittings was however rather poor. By measuring frequency separations between $Q_{1,2}$ and $P_{1,2}$ transitions for (e) and (f) Λ -doublet states we were able to derive sums and differences of Λ -doublet splittings in the $A^2\Delta$ state for $N = 8, 9, 12$, and 13 for both F_1 and F_2 states.

II. EXPERIMENT

The molecular beam machine, including the CH production source and the LIF zone, is the same as used in the

previous investigation on the high resolution spectrum of the $C^2\Sigma^+ \leftarrow X^2\Pi$ transition of CH.¹¹ The molecules were excited by about 5 mW of the reduced output power at $\lambda = 430$ nm of a stabilized dye laser, driven on stilbene pumped by 1,5 W UV power from an Ar-ion laser. The molecular beam was chopped at 120 Hz and the signal to noise ratio of the CH line spectra, detected by a lock-in with integration (RC) time 0.3 s, was over 20 also for the higher rotational states. With the experimental linewidth of 20 MHz the different hyperfine components were completely resolved. In a second molecular beam machine NO_2 molecules were simultaneously detected with a spectral linewidth of 10 MHz. The dense NO_2 spectrum contains in average more than one line per GHz and was used to make overlapping scans of each 25 GHz of the laser. In this way frequency separations of 200 GHz could be measured in terms of the calibrated free spectral ranges ($\text{FSR} = 149.605 \pm 0.015$ MHz) of a pressure and temperature stabilized interferometer.¹²

III. HYPERFINE STRUCTURE

The hyperfine splittings of the four lowest rotational states in both F_1 and F_2 ladders of the $A^2\Delta$ state have been measured and analyzed by Brazier and Brown.⁴ As a result they obtained accurate values for the hyperfine parameters a , b , and c of Frosch and Foley that describe the observed splittings very well within the experimental error limits. In the present investigation the high rotational temperature ($T_{\text{rot}} \sim 800$ K) in the molecular CH beam¹¹ and the high spectral resolution (20 MHz) allowed for accurate measurements of hyperfine splittings up to $N = 14$. The observed frequency separations between hyperfine doublet components of several lines of $Q_{1,2}$ and $P_{1,2}$ branches are listed in Table I. The observed hyperfine doublets contain four transitions (in the P branches three) between hyperfine states in $X^2\Pi$ and $A^2\Delta$ of which two (in the P branches one) are very weak. In Table II, and separately for the strongly perturbed $N = 10$ states in Table III, the hyperfine splittings of rotational states in F_1 and F_2 ladders of $A^2\Delta$ are given, as derived from the observed splittings by taking into account the hyperfine splitting in the $X^2\Pi$ state. Because we did not observe differences in hyperfine splittings between both parity states average values were taken, except for the $N = 10$ level, for reasons given below. In Fig. 1 recorded spectra of both parity transitions of $Q_1(10)$ and $Q_2(10)$ are shown. The

TABLE I. Observed hyperfine splittings (in MHz) for CH in the $A^2\Delta$, $v=0 \leftarrow X^2\Pi$, $v=0$ transitions, for (e) and (f) states.

Transition	Obs. Splitting (e)	Obs. Splitting (f)
$Q_1(6)$	387.3 ± 2.0	362.5 ± 2.0
$Q_1(7)$	385.2 ± 1.5	361.7 ± 1.5
$Q_2(7)$	257.1 ± 1.5	278.2 ± 1.5
$Q_1(8)$	385.0 ± 1.5	361.1 ± 2.0
$Q_2(8)$	254.8 ± 1.5	276.7 ± 1.5
$Q_1(9)$	396.4 ± 1.5	377.8 ± 1.5
$Q_2(9)$	240.8 ± 2.0	263.8 ± 2.0
$P_1(9)$	385.8 ± 2.0	362.5 ± 2.0
$P_2(9)$	254.9 ± 2.0	276.8 ± 2.0
$Q_1(10)$	590.4 ± 2.0	586.3 ± 4.5
	66.8 ± 1.5	50.5 ± 2.5
$Q_2(10)$	579.5 ± 3.0	590.1 ± 4.0
	26.2 ± 4.5	
$Q_1(11)$	318.8 ± 2.0	302.1 ± 2.0
$Q_2(11)$		342.2 ± 2.0
$P_1(11)$	588.8 ± 3.0	587.8 ± 3.0
	74.5 ± 3.0	49.5 ± 3.0
$P_2(11)$	574.3 ± 2.0	587.0 ± 3.0
	14.0 ± 3.0	
$Q_1(12)$	335.1 ± 2.5	315.6 ± 2.5
$Q_1(13)$	342.6 ± 1.5	322.8 ± 2.0
$Q_2(13)$	292.6 ± 2.0	324.8 ± 2.0
$P_1(13)$	318.1 ± 2.0	338.7 ± 2.0
$P_2(13)$	325.1 ± 2.5	306.6 ± 2.5
$Q_1(14)$	343.1 ± 2.5	329.5 ± 4.0
$Q_2(14)$	300.8 ± 1.5	359.9 ± 4.0

large frequency separations, the triplet structure, and the intensity distribution for the $Q_{1,2}(10)$ lines, that appear also in the $P_{1,2}(11)$ transition, indicate that there is an irregularity in the hyperfine structure for the $N=10$ states. Also the splittings for $N=7$ to $N=14$ deviate from expected values

TABLE II. Hyperfine splittings (in MHz) for CH in the $A^2\Delta$, $v=0$, N states.

State	Measured	Calculated	Obs. - Calc.
$F_1, N=2$	448.0 ± 1.5	446.6	1.3 ^a
$N=3$	401.4 ± 1.5	398.6	2.7 ^a
$N=4$	369.2 ± 1.5	373.1	-3.9 ^a
$N=5$	359.2 ± 1.5	357.8	1.4 ^a
$N=6$	343.0 ± 1.5	348.3	-5.3
$N=7$	341.0 ± 1.5	343.1	-2.1
$N=8$	340.4 ± 1.5	342.8	-2.4
$N=9$	354.9 ± 1.5	355.5	-0.6
$N=11$	276.2 ± 3.0	274.0	2.2
$N=12$	292.9 ± 1.5	291.0	1.9
$N=13$	297.9 ± 1.5	295.2	2.7
$N=14$	299.7 ± 1.5	296.4	3.3
$F_2, N=2$	159.6 ± 1.5	160.2	-0.6 ^a
$N=3$	183.6 ± 1.5	185.3	-1.7 ^a
$N=4$	203.5 ± 1.5	202.1	1.4 ^a
$N=5$	216.7 ± 1.5	213.2	3.5 ^a
$N=7$	222.4 ± 1.5	224.0	-1.6
$N=8$	221.4 ± 1.5	223.3	-1.9
$N=9$	208.7 ± 1.5	209.9	-1.2
$N=11$	289.0 ± 3.0	290.5	-1.5
$N=12$	274.0 ± 1.5	273.2	0.8
$N=13$	268.1 ± 1.5	268.8	-0.7
$N=14$	270.8 ± 1.5	267.5	3.3

^a From Ref. 4.

TABLE III. Hyperfine splittings (in MHz) in $N=10$ rotational states of $A^2\Delta$ for both parity states + and -.

	Measured Splitting	Calc. Splitting	Obs. - Calc.
+ parity			
$F=10-F=10$	587.6 ± 3.0	589.5	-1.9
$F=11-F=10$	28.6 ± 3.0	29.3	-0.7
$F=10-F=9$	56.0 ± 4.0	53.9	2.1
- parity			
$F=10-F=10$	591.8 ± 2.0	589.4	2.4
$F=11-F=10$	24.1 ± 2.0	25.9	-1.8
$F=10-F=9$	53.5 ± 4.0	50.4	3.1

that were calculated in first order perturbation theory from the hyperfine constants of Brazier and Brown.⁴

The hyperfine structure in CH ($A^2\Delta$) is caused by the interaction between the nuclear spin I of the proton and the net electronic spin S and orbital angular momentum L . The Hamiltonian appropriate for the present investigation is

$$H_{\text{hf}} = a \mathbf{I} \cdot \mathbf{L} + b \mathbf{I} \cdot \mathbf{S} + c I_x S_x. \quad (1)$$

Usually this interaction can be considered as a small perturbation with respect to the rotational energy splittings so that the hyperfine splittings are well explained by calculating only the matrix elements diagonal in the rotational states. In this particular case, however, the rotational states of the $^2\Delta_{3/2}$ and $^2\Delta_{5/2}$ ladders approach each other so closely that their off-diagonal interaction can no longer be neglected. From molecular constants of the $A^2\Delta$ state, as derived by Brazier and Brown⁴ from absolute frequencies of $A^2\Delta \leftarrow X^2\Pi$ transitions, a crossing between the $^2\Delta_{3/2}$ and $^2\Delta_{5/2}$ ladders within a less than 100 MHz separation is to be expected at $N=14$. Unfortunately the published value of the spin-rotation coupling constant γ was erroneous, due to a misprint¹³; with the correct value $\gamma = 0.0422 \pm 0.0002 \text{ cm}^{-1}$ the crossing is predicted at $N=10$ in agreement with the present experiment. In Fig. 2 the structure of interacting levels of $^2\Delta_{3/2}$ and $^2\Delta_{5/2}$ rotational states is represented schematically.

By the hyperfine interaction (1), two levels with the same F value and parity repel each other when they are close together. The repelling depends on the hyperfine free energy difference $\Delta_{\pm} E$ between $^2\Delta_{3/2}$ and $^2\Delta_{5/2}$,

$$\Delta_{\pm} E(N) = E_{\pm}(\Delta_{3/2}, N) - E_{\pm}(\Delta_{5/2}, N), \quad (2)$$

that is positive for $N < 10$ and negative for $N > 10$; the subscript \pm indicates parity of Λ -doublet states.

The rotational eigenfunctions for the $^2\Delta$ state can be expressed in symmetrized Hund's case (a) basis functions:

$$\begin{aligned}
 |^2\Delta_{\Omega} JIFM_F\rangle \\
 = C_{\Omega,3/2}(J) [|^2\Delta_{3/2} JIFM_F\rangle_a + p|^2\Delta_{-3/2} JIFM_F\rangle_a] \\
 + C_{\Omega,5/2}(J) [|^2\Delta_{5/2} JIFM_F\rangle_a + p|^2\Delta_{-5/2} JIFM_F\rangle_a], \quad (3)
 \end{aligned}$$

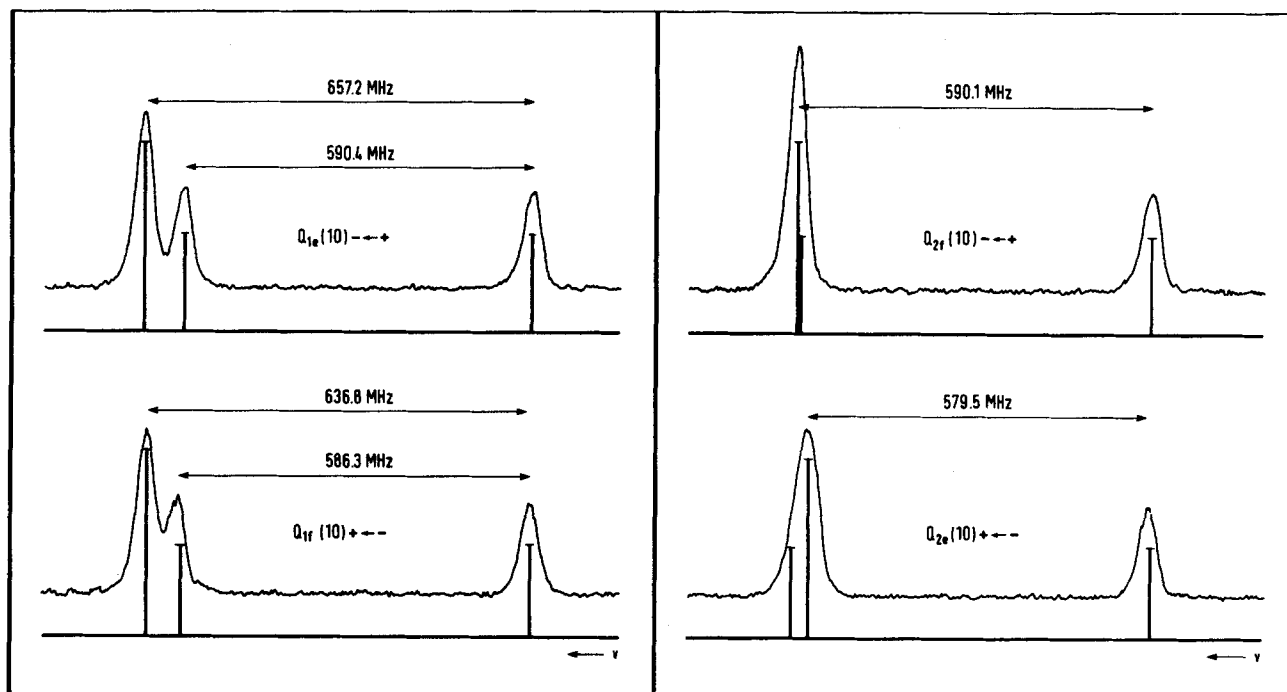


FIG. 1. Observed spectrum for $Q_1(10)$ and $Q_2(10)$ transitions. The sticks represent relative frequency splittings and line intensities of the calculated spectrum.

where p indicates the symmetry of the electronic wave function; the mixing coefficients $C_{\Omega,\Omega'}(J)$ are obtained by diagonalizing the rotation matrix of the $A^2\Delta$ state as given in Eq. (4). On the basis of Slater determinant wave functions¹⁴ one can deduce a relation between p and the total parity of the states. For both $\Omega = 3/2$ and $\Omega = 5/2$ the reflection operator σ_{xz} yields

$$\sigma_{xz} |^2\Delta_{\Omega} J M p\rangle = p(-)^{J+1/2} |^2\Delta_{\Omega} J M p\rangle \quad (4)$$

so the total parity is $p(-)^{J+1/2}$. In the terminology of Ref. 4 symmetric and antisymmetric wave functions correspond to (f) and (e) states, respectively.

Matrix elements M_{ij} of the hyperfine Hamiltonian H_{hf} in the representation of Eq. (3) are

$$\begin{aligned} M_{11} &= \frac{-1}{2(J+1)} \left[\frac{3}{2} C_{5/2,3/2}^2(J) \{ -2a + \frac{1}{2}(b+c) \} - \frac{3}{2} C_{5/2,5/2}^2(J) \{ 2a + \frac{1}{2}(b+c) \} \right. \\ &\quad \left. - C_{5/2,3/2}(J) C_{5/2,5/2}(J) \sqrt{(J-3/2)(J+5/2)} b \right], \\ M_{22} &= -\frac{(J+1)}{J} M_{11}, \\ M_{33} &= \frac{-1}{2J} \left[\frac{3}{2} C_{3/2,3/2}^2(J-1) \{ -2a + \frac{1}{2}(b+c) \} - \frac{3}{2} C_{3/2,5/2}^2(J-1) \{ 2a + \frac{1}{2}(b+c) \} \right. \\ &\quad \left. - C_{3/2,5/2}(J-1) C_{3/2,3/2}(J-1) \sqrt{(J-5/2)(J+3/2)} b \right], \\ M_{44} &= \frac{-J}{J-1} M_{33}, \\ M_{23} &= \frac{1}{2\sqrt{2}J} \left[C_{5/2,3/2}(J) C_{3/2,3/2}(J-1) \sqrt{2(J+3/2)(J-3/2)} \{ -2a + \frac{1}{2}(b+c) \} \right. \\ &\quad - C_{5/2,5/2}(J) C_{3/2,5/2}(J-1) \sqrt{2(J+5/2)(J-5/2)} \{ 2a + \frac{1}{2}(b+c) \} \\ &\quad - \{ C_{5/2,3/2}(J) C_{3/2,5/2}(J-1) \sqrt{(J-5/2)(J-3/2)} \\ &\quad \left. - C_{5/2,5/2}(J) C_{3/2,3/2}(J-1) \sqrt{(J+3/2)(J+5/2)} \} \frac{1}{2} \sqrt{2} b \right], \\ M_{32} &= M_{23}. \end{aligned} \quad (5)$$

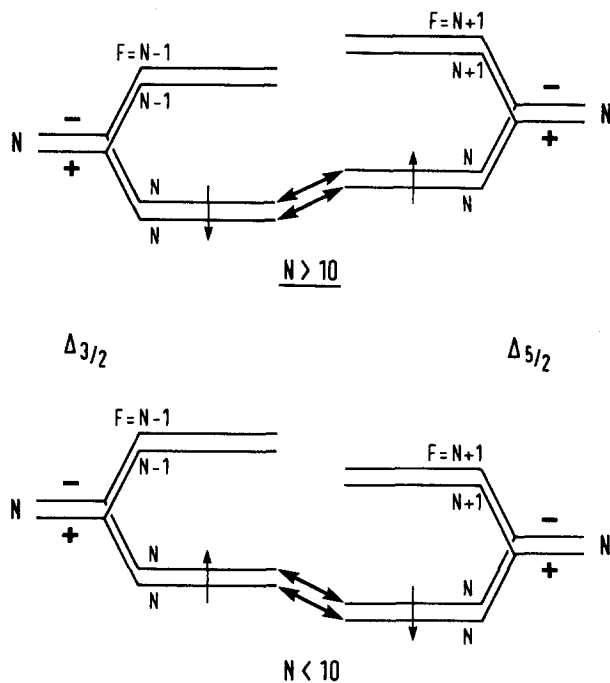


FIG. 2. Hyperfine interaction between $\Delta_{5/2}$ and $\Delta_{3/2}$ states of CH. The up and down pointing arrows show the repelling of resonant states with equal quantum numbers. The parities are arbitrarily chosen.

The structure of the matrix is shown schematically in Table IV. The off-diagonal matrix elements represent the coupling between hyperfine states with equal F and parity of both spin-orbit ladders, which cause the irregularity in the hyperfine structure. Diagonalization of the matrix in Table IV yields the perturbed hyperfine splittings. In a least squares fit incorporating the reported data⁴ of rotational states $N = 2$ to $N = 5$ and the present results, we obtained new values for the a , b , and c hyperfine constants as listed in Table V. Only the a constant undergoes a change larger than the error limits with respect to the values of Brazier and Brown.⁴ Recent many-body calculations of hyperfine constants by Kristianson and Veseth¹⁵ show very good agreement for the a and c constants, while the b constant differs only 10% from the experimental value. The hyperfine splittings calculated with these constants are in good agreement with the measured values as shown in Tables II and III. In Fig. 3 the resonance is shown schematically in a plot of perturbed and unperturbed hyperfine splittings around $N = 10$.

For the $N = 10$ states the strong perturbations are explained by very small energy separations between the "hyperfine free" states. From a least squares fit of the measured splittings we obtained

TABLE IV. Matrix representation for the hyperfine interaction.

$^2\Delta_{5/2}, J, p$		$^2\Delta_{3/2}, J-1, -p$	
$F = J + 1/2$	$F = J - 1/2$	$F = J - 1/2$	$F = J - 3/2$
M_{11}	0	0	0
0	M_{22}	M_{23}	0
0	M_{32}	$M_{33} + \Delta E$	0
0	0	0	$M_{44} + \Delta E$

TABLE V. Proton hyperfine constants (in MHz) for the $A^2\Delta$ state of CH.

	Present	Ref. 4	Ref. 15
a	55.00 ± 0.43	57.26 ± 0.85	53.91
b	562.68 ± 0.79	563.6 ± 3.4	526.3
c	61.1 ± 2.4	61.4 ± 8.0	61.6

$$\Delta_+ E(10) = -61.0 \pm 4.3 \text{ MHz},$$

$$\Delta_- E(10) = -54.0 \pm 4.8 \text{ MHz}.$$

From the unperturbed energy matrix of Ref. 4, we calculated that the $F = 10$ hyperfine states would lie as closely as 10 MHz apart; the hyperfine interaction (1) causes the $F = 10$ states to be moved from each other over nearly 600 MHz. The calculated eigenfunctions are completely mixed up and give rise to stick spectra which are in good agreement with the measurement as shown in Fig. 1.

IV. Λ DOUBLING

In several tedious but carefully performed overlapping continuous scans of 25 GHz each, we measured frequency separations $\Delta\nu_{P,Q}$ between rotational transitions originating in (e) and (f) states of $Q_{1,2}$ and $P_{1,2}$ branches for $N = 9$ and 13. In the overlapping procedure small corrections were made for the drift of the interferometer during the time that it took to set the laser at the desired start frequency. The overlapping points could be determined very accurately because of the small linewidths (10 MHz) of the NO_2 lines that were simultaneously detected by LIF in a second machine with a highly collimated molecular beam. In this way frequency splittings $\Delta\nu(N)$ between (e) and (f) transitions were obtained in terms of markers of a stabilized interferometer, a method that is in principle much more accurate than trying to deduce Λ splittings from differences of absolute wavelengths of (e) and (f) transitions. The errors in the $\Delta\nu$ values as listed in Table VI are estimated 30 MHz; all splittings were measured by scanning frequency once up and once down, and the observed values did not differ more than 15 MHz.

TABLE VI. Observed splittings (in MHz) between (e) and (f) components of $A^2\Delta$ transitions. The values under (l) and (u) refer to the lower and upper component of the resolved hyperfine doublets. The estimated errors are 30 MHz.

Transition	Obs. Splitting (l)	Obs. Splitting (u)
$Q_1(9)$	95 297.6	95 277.2
$P_1(9)$	95 272.5	95 249.2
$Q_2(9)$	104 586.6	104 570.2
$P_2(9)$	104 589.8	104 562.6
$Q_1(13)$	189 277.1	189 259.1
$P_1(13)$	189 196.0	189 176.4
$Q_2(13)$	202 084.5	202 054.7
$P_2(13)$	202 103.2	202 082.9

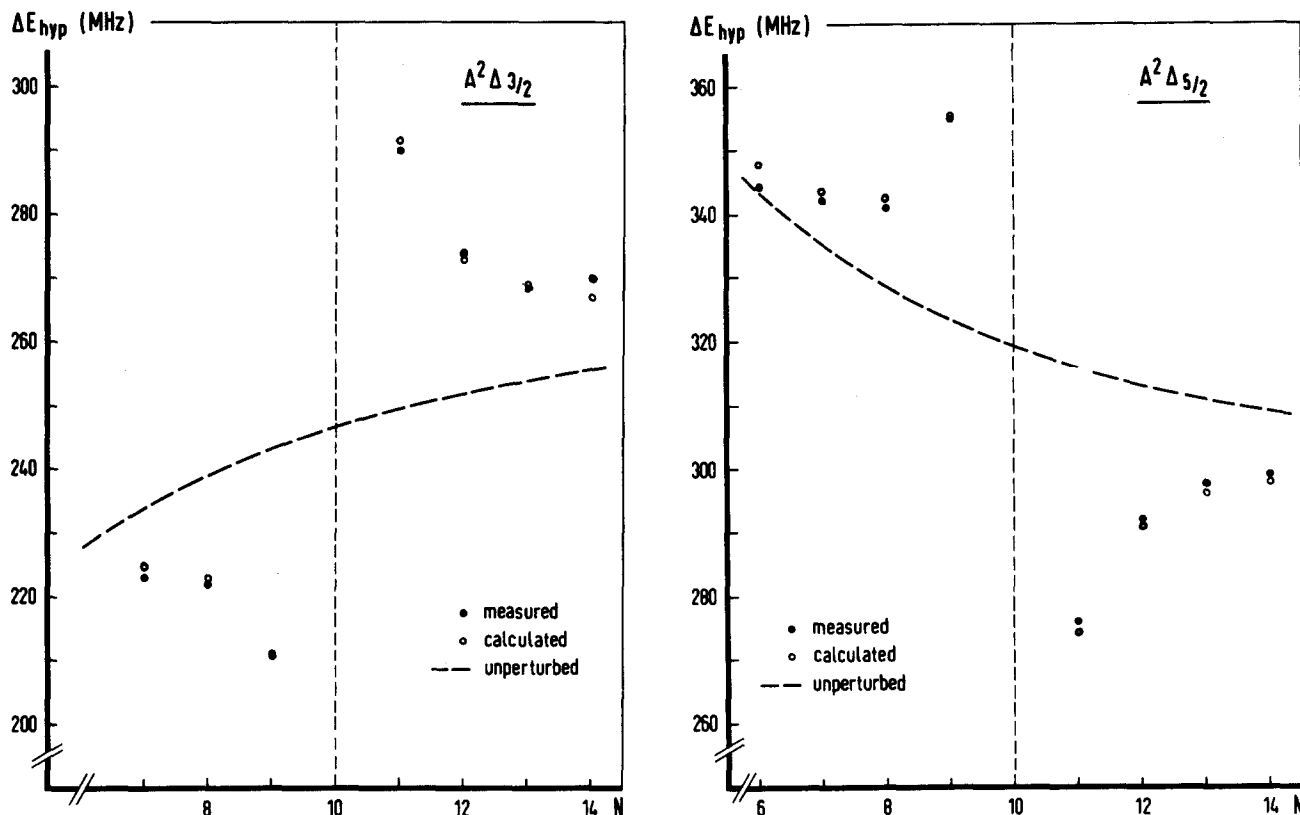


FIG. 3. Observed and calculated hyperfine splittings in the $\Delta_{5/2}$ and $\Delta_{3/2}$ states of CH around the hyperfine resonance at $N = 10$.

The measured values $\Delta\nu(N)$ are combinations of Λ splittings $\Delta\Lambda$ in the $X^2\Pi$ ground state and for a very small part in the excited $A^2\Delta$ state:

$$\begin{aligned}\Delta\nu_{Q_1}(N) &= \Delta\Lambda(\Delta_{5/2}, N) + \Delta\Lambda(\Pi_{1/2}, N), \\ \Delta\nu_{P_1}(N) &= -\Delta\Lambda(\Delta_{5/2}, N-1) + \Delta\Lambda(\Pi_{1/2}, N), \\ \Delta\nu_{Q_2}(N) &= \Delta\Lambda(\Delta_{3/2}, N) + \Delta\Lambda(\Pi_{3/2}, N), \\ \Delta\nu_{P_2}(N) &= -\Delta\Lambda(\Delta_{3/2}, N-1) + \Delta\Lambda(\Pi_{3/2}, N); \quad (6)\end{aligned}$$

it is assumed that the upper Λ -doublet levels are of e type in the F_1 ladder and of f type in the F_2 ladder (see below). By subtracting the measured $\Delta\nu$ values of Table VI,

$$\begin{aligned}\Delta\nu_{Q_1}(N) - \Delta\nu_{P_1}(N) &= \Delta\Lambda(\Delta_{5/2}, N) + \Delta\Lambda(\Delta_{5/2}, N-1), \\ \Delta\nu_{Q_2}(N) - \Delta\nu_{P_2}(N) &= \Delta\Lambda(\Delta_{3/2}, N) + \Delta\Lambda(\Delta_{3/2}, N-1), \quad (7)\end{aligned}$$

we find the sums of Λ splittings for successive N states in $A^2\Delta$ as listed in Table VII.

In comparison with Π states the Λ doubling in Δ states is a very small effect. It originates in the spin-orbit and Coriolis interaction with nearby lying Σ states via intermediate Π

states. The effect can be taken into account in the rotation matrix via the introduction of the Λ doubling parameters p_Δ and q_Δ for the $A^2\Delta$ state as deduced by Brazier and Brown.⁴ By diagonalization we find the approximate expression for the Λ -doublet splittings:

$$\begin{aligned}\Delta\Lambda(\Delta_{5/2}, N) &= N(N+1)(N+2)[\tfrac{1}{2}(p+4q) - q(N+1)], \\ \Delta\Lambda(\Delta_{3/2}, N) &= -(N-1)N(N+1)[\tfrac{1}{2}(p+4q) + qN]. \quad (8)\end{aligned}$$

In the assumption that the p and q parameters do not differ by more than an order of magnitude we expect that certainly for higher N states the e - f ordering in the F_1 and F_2 ladders is different. This conclusion can also be drawn from the results for $\Delta_\pm E(10)$ in the analysis of the hyperfine resonance; the almost equal values for $\Delta_+ E(10)$ and $\Delta_- E(10)$ indicate that the $N = 10$ upper (or lower) states have the same parity and are thus of different e - f type. From the result for $N = 12$ and 13 in $\Delta_{5/2}$ we conclude that the upper Λ -doublet levels of the e type in the F_1 ladder and consequently of f type in the F_2 ladder. We have no explanation for the negative result for $N = 12$ and 13 in $\Delta_{3/2}$, although it is not inconsistent in view of the experimental error of 50 MHz.

Unfortunately the resulting Λ -doublet splittings are too small, compared to the errors to deduce the p_Δ and q_Δ Λ -doublet constants for the $A^2\Delta$ state. The reason for starting this part of the experiment was the expectation, from reported constants,⁴ that at $N = 13$ the Λ -doublet splittings should be of the order of 300 MHz. From the present experiment, in which the experimental accuracy is better, we conclude how-

TABLE VII. Derived sums of Λ splittings (in MHz) for the $A^2\Delta$ state of CH.

$\Lambda(\Delta_{5/2}, 12) + \Lambda(\Delta_{5/2}, 13) =$	81.9 ± 50
$\Lambda(\Delta_{3/2}, 12) + \Lambda(\Delta_{3/2}, 13) =$	-23.5 ± 50
$\Lambda(\Delta_{5/2}, 8) + \Lambda(\Delta_{5/2}, 9) =$	26.5 ± 50
$\Lambda(\Delta_{3/2}, 8) + \Lambda(\Delta_{3/2}, 9) =$	2.2 ± 50

ever that the Λ -doublet splittings for $N = 13$ are less than 70 MHz, and that the reported values for p_Δ and q_Δ are at least a factor of 3 too high.

V. CONCLUSION

The observed hyperfine resonance between $\Delta_{5/2}$ and $\Delta_{3/2}$ ladders at $N = 10$ is probably the first of its kind in a diatomic molecule in a non- Σ state. In their investigation of the perturbation in the $X^4\Sigma^-$ state of VO, Richards and Barrow⁷ state that internal hyperfine perturbations are limited to Hund's case (b) coupling cases and in particular to Σ states of high multiplicity. The presently observed perturbation occurs however in a $^2\Delta$ state. Indeed the $A^2\Delta$ state of CH has a small A/B value, so the coupling case is almost case (b).

The fact that the resonance feature is so pronounced, the hyperfine structure being so heavily perturbed at $N = 10$, is a consequence of the very small energy difference (about 10 MHz) between $F = 10$ hyperfine states in F_1 and F_2 ladders when calculated for the unperturbed case. The fact that the energy splitting between the two spin-orbit ladders at $N = 10$ is so small (< 10 MHz) is therefore purely accidental.

The Λ doubling in Δ states is known to be very small. Until now the only accurate determination of the Λ doubling in a Δ state was carried out for the metastable $a^1\Delta$ state of NH.¹⁶ In comparison with NH the Λ doubling for CH($A^2\Delta$) is about four times smaller. Even though the Λ splittings are proportional with N^4 they are very small for N values up to 13. Maybe in the future they might be measured

more accurately by double resonance techniques in the excited state.

ACKNOWLEDGMENTS

The authors would like to thank Mr. H. Caspers for his help in the analysis of the Λ -doubling spectra and Professor J. Brown (Oxford University) for his advice. We want to show gratitude to the referee who drew attention to the hyperfine perturbations in vanadium oxide.

- ¹O. E. H. Rydbeck, J. Ellder, and W. M. Irvine, *Nature* **246**, 466 (1973).
- ²B. E. Turner and B. Zuckerman, *Astrophys. J.* **187**, L59 (1974).
- ³M. Bogey, C. DeMuyneck, and J. L. Destombes, *Chem. Phys. Lett.* **100**, 105 (1983).
- ⁴C. R. Brazier and J. M. Brown, *Can. J. Phys.* **62**, 1563 (1984).
- ⁵K. M. Evenson, H. E. Radford, and M. M. Moran, Jr., *Appl. Phys. Lett.* **18**, 426 (1971).
- ⁶L. Gero, *Z. Phys.* **117**, 709 (1941).
- ⁷D. Richards and R. F. Barrow, *Nature* **219**, 1244 (1968).
- ⁸W. H. Hocking, A. J. Merer, and D. J. Milton, *Can. J. Phys.* **59**, 266 (1981).
- ⁹A. S.-C. Cheung, R. C. Hansen, A. M. Lyyra, and A. J. Merer, *J. Mol. Spectrosc.* **86**, 526 (1981).
- ¹⁰R. M. Gordon and A. J. Merer, *Can. J. Phys.* **58**, 642 (1980).
- ¹¹W. Ubachs, G. Meyer, J. J. ter Meulen, and A. Dymanus, *J. Chem. Phys.* **84**, 3032 (1986).
- ¹²J. P. Bekooij, W. L. Meerts, and A. Dymanus, *J. Mol. Spectrosc.* **102**, 320 (1983).
- ¹³J. M. Brown (private communication).
- ¹⁴W. Ubachs, J. J. ter Meulen, and A. Dymanus, *Can. J. Phys.* **62**, 1374 (1984).
- ¹⁵L. Veseth (private communication).
- ¹⁶W. Ubachs, G. Meyer, J. J. ter Meulen, and A. Dymanus, *J. Mol. Spectrosc.* **115**, 88 (1986).